Inhibitory Role of Peroxisome Proliferator-Activated Receptor Gamma in Hepatocarcinogenesis in Mice and *In Vitro*

Jun Yu,[1] Bo Shen,[1] Eagle S. H. Chu,[1] Narci Teoh,[2] Kin-Fai Cheung,[1] Chung-Wah Wu,[1] Shiyan Wang,[1] Cleo N. Y. Lam,[1] Hai Feng,[1] Junhong Zhao,[1] Alfred S. L. Cheng,[1] Ka-Fai To,[3] Henry L. Y. Chan,[1] and Joseph J. Y. Sung[1]

Although peroxisome proliferator-activated receptor gamma (PPARγ) agonist have been shown to inhibit hepatocellular carcinoma (HCC) development, the role of PPARγ in hepatocarcinogenesis remains unclear. We investigated the therapeutic efficacy of PPARγ against HCC. PPARγ-deficient ($PPAR\gamma^{+/-}$) and wild-type ($PPAR\gamma^{+/+}$) littermates were used in a diethylnitrosamine (DEN)-induced HCC model and treated with PPARγ agonist (rosiglitazone) or the vehicle alone for 8 months. The effects of PPARγ on HCC cell growth and apoptosis were examined using PPARγ-expressing adenovirus (Ad-PPARγ). $PPAR\gamma^{+/-}$ mice were more susceptible to DEN-induced HCC than $PPAR\gamma^{+/+}$ mice (94% versus 62%, $P < 0.05$), and rosiglitazone significantly reduced the incidence of HCC in $PPAR\gamma^{+/+}$ mice (vehicle 62% versus treatment 24%, $P < 0.01$), but not in $PPAR\gamma^{+/-}$ mice, indicating that PPARγ suppresses hepatocellular carcinogenesis. A pronounced expression of PPARγ was observed in a HCC cell line (Hep3B) infected with Ad-PPARγ. Such induction markedly suppressed HCC cell viability ($P < 0.01$). Further, Hep3B infection with Ad-PPARγ revealed a decreased proportion of cells in S-phase (12.92% versus 11.58%, $P < 0.05$), with arrest at G_2/M phase (38.2% versus 55.68%, $P < 0.001$), and there was concomitant phosphorylation of the key G_2/M phase inhibitors cdc25C and cdc2. PPARγ overexpression increased cell apoptosis (21.47% versus 35.02%, $P < 0.01$), mediated by both extrinsic (Fas and tumor necrosis factor-α) and intrinsic (caspase-9, caspase-3, caspase-7, and poly[ADP-ribose] polymerase) pathways. Moreover, PPARγ directly induced a putative tumor suppressor gene, growth differentiation factor-15. *Conclusion:* Loss of one PPARγ allele is sufficient to enhance susceptibility to HCC. PPARγ suppresses tumor cell growth through reducing cell proliferation and inducing G_2/M phase arrest, apoptosis, and up-regulating growth differentiation factor-15. Thus, PPARγ acts as a tumor-suppressor gene in the liver. (HEPATOLOGY 2010;51:2008-2019)

Hepatocellular carcinoma (HCC) remains the third leading cause of cancer death worldwide.[1] The prognosis of HCC is poor with mortality almost equalling incidence[1] with limited effective treatment options. Thus, there is a compelling need for a novel strategy that will improve the treatment of HCC and ultimately increase the survival of patients with HCC.

Abbreviations: ACOX, acyl-coenzymeA oxidases; Ad-PPARγ, adenovirus-expressing PPARγ; APAF, apoptotic protease activating factor; cDNA, complementary DNA; ChIP, chromatin immunoprecipitation; DEN, diethylnitrosamine; FACS, fluorescence-activated cell sorting; Fn, fibronectin; GDF15, growth differentiation factor 15; HCC, hepatocellular carcinoma; MOI, multiplicity of infection; PARP, nuclear enzyme poly(ADP-ribose) polymerase; PCNA, proliferating cell nuclear antigen; PCR, polymerase chain reaction; PI, propidium iodide; PPARγ, peroxisome proliferator-activated receptor gamma; PTEN, phosphatase and tensin homolog; TBXA2R, thromboxane A2 receptor; TNF, tumor necrosis factor; TUNEL, terminal deoxynucleotidyl transferase-mediated dUTP nick-end labeling; WT, wild-type.

From the [1]Institute of Digestive Disease and Department of Medicine and Therapeutics, Li Ka Shing Institute of Health Sciences, Hong Kong, China; [2]Australian National University Medical School at the Canberra Hospital, Canberra, Australia; and [3]Department of Anatomical and Cellular Pathology, the Chinese University of Hong Kong, Hong Kong, China.

Received August 21, 2009; accepted January 5, 2010.

The project was supported by Research Grants Council Competitive Earmarked Research Grant CUHK 478207 and by Research Grants Council Competitive Earmarked Research Grant CUHK 478108.

Address reprint requests to: Jun Yu, Institute of Digestive Disease, Department of Medicine and Therapeutics, Prince of Wales Hospital, the Chinese University of Hong Kong, Shatin, NT, Hong Kong, China. E-mail: junyu@cuhk.edu.hk; fax: (852) 21445330.

The peroxisome proliferator-activating receptor γ (PPARγ) is a member of the nuclear receptor superfamily of transcription factors. The role of PPARγ in the onset and treatment of cancer has been the focus of recent attention. PPARγ agonists inhibit the proliferative activity of neoplastic cells, suppress the growth of human tumor xenografts in nude mice,[2,3] and reduce the frequency of spontaneous and carcinogen-induced preneoplastic and neoplastic lesions in animals,[2-5] which is indicative of the tumor suppressor effects of PPARγ.[2] These observations have prompted phase II clinical trials using PPARγ agonists as novel therapy for patients with liposarcoma, colon, breast, and prostate cancer.[5,6] Our group and others have previously demonstrated the antitumorigenic effects of PPARγ agonists in several liver cancer cell lines.[7,8] PPARγ agonist stimulation induced cell cycle arrest and apoptosis and inhibited the growth of liver cancer cells.[9-12] Thus, these findings support the hypothesis that PPARγ may act as a potent tumor suppressor in hepatocarcinogenesis. Of note, the antitumor effects of PPARγ agonists may be mediated via PPARγ-dependent and PPARγ-independent pathways,[2,13] but the role of PPARγ itself in hepatocarcinogenesis is still unclear.

To elucidate the role of PPARγ in its therapeutic efficacy against HCC, diethylnitrosamine (DEN) was used to induce primary liver cancer in PPARγ wild-type (PPAR$\gamma^{+/+}$) and PPARγ heterozygous-deficient (PPAR$\gamma^{+/-}$) mice, followed by treatment with the PPARγ agonist rosiglitazone. We also examined the functional significance of endogenous PPARγ overexpression in human HCC cells using an adenovirus-PPARγ construct.

Materials and Methods

Animals and Experimental Design. All homozygous PPARγ knockout animals were embryonically lethal due to placental dysfunction. We therefore used PPARγ heterozygous-deficient mice (PPAR$\gamma^{+/-}$) in this study. PPARγ-deficient (PPAR$\gamma^{+/-}$) mice were kindly supplied by Professor Frank J. Gonzalez (Center for Cancer Research, National Cancer Institute, Bethesda, MD). The generation of the transgenic mice was described previously.[9] Genotyping was done by means of polymerase chain reaction (PCR). Animals were housed in an air-conditioned room under a 12-hour light/12-hour dark cycle and allowed free access to food and water.

Mice of age 15 days received a single intraperitoneal injection of DEN (5 mg/kg body weight; Sigma Chemical Co., St. Louis, MO) and then were randomly treated with or without the selective PPARγ agonist rosiglitazone (200 ppm) in their food (GlaxoSmithKline, Research Triangle Park, NC) for up to 8 months for male mice and 10 months for female mice. Because of known sex differences that could confound HCC development, our subsequent studies were confined to male mice only. The numbers of mice in the four experimental groups were: group 1 (PPAR$\gamma^{+/+}$ mice received DEN), 13; group 2 (PPAR$\gamma^{+/-}$ mice received DEN), 17; group 3 (PPAR$\gamma^{+/+}$ mice received DEN and rosiglitazone), 14; and group 4 (PPAR$\gamma^{+/-}$ mice received DEN and rosiglitazone), 13. At the end of treatments, blood was collected by cardiac puncture under anesthesia. Livers were rapidly excised and weighed. The presence and dimensions of surface nodules were evaluated and recorded. Liver was cut into strips of 2-3 mm thickness to examine the presence of macroscopically visible lesions. HCCs were confirmed histologically by an experienced pathologist (K.F.T.) from either grossly or histologically evident nodules. The appearance of adenoma or high-grade dysplasia nodule was not accounted in this study. All experiments in the current study were conducted in accordance with guidelines by the Animal Experimentation Ethics Committee of the Chinese University of Hong Kong.

Human HCC Cell Culture. The human HCC cell line (Hep3B) was obtained from the American Type Culture Collection (ATCC, Manassas, VA). Hep3B cells were cultured in Dulbecco's modified Eagle medium with 10% fetal bovine serum (Invitrogen, Carlsbad, CA) and penicillin (200 U/mL), and were maintained at 37°C in a humidified atmosphere with 5% CO_2.

Adenovirus-Mediated PPARγ Gene Transfer. Recombinant adenovirus containing the mouse PPARγ1 complementary DNA (cDNA) (Ad-PPARγ) under regulation of the cytomegalovirus (CMV) promoter, and recombinant adenovirus containing *E. coli* β-galactosidase gene (Ad-LacZ) as control adenovirus vector were generous gifts from Dr. J. K. Reddy (Department of

Published online in Wiley InterScience (www.interscience.wiley.com).
DOI 10.1002/hep.23550
Potential conflict of interest: Nothing to report.
Additional Supporting Information may be found in the online version of this article.

Pathology, the Feinberg School of Medicine, Northwestern University, Chicago).

Adenovirus was propagated, isolated in human embryonic kidney 293 (HEK293) cells, and purified with Adeno-X Virus Purification kit (Clontech, Mountain View, CA). Titer of the viral solution was determined by Adeno-X Rapid Titer kit (Clontech). The virus with titer range from 1.0×10^9 to 1.0×10^{10} plaque forming units (pfu)/mL was stored at −80°C until use. Adenoviral infections were carried out at various multiplicities of infection (MOI) which was determined by monitoring cytopathic effect after transfection. The transfection effect was monitored and counted for X-gal (bromo-chloro-indolyl-galactopyranoside) staining under microscope.

X-gal Staining. X-gal staining was performed to confirm LacZ gene transduction according to the manufacturer's instructions (X-gal Staining Assay Kit; Genlantis, San Diego, CA).

Construction of Growth Differentiation Factor 15 Expression Vector and Transient Transfection. The entire coding sequence of growth differentiation factor 15 (GDF15) cDNA was cloned and inserted into the pCMV6 vector (OriGene, Rockville, MD). Hep3B cells were grown to 70%-90% confluence. The pCMV6-GDF15 and control vector (pCMV6) were then added to culture medium along with Lipofectamine 2000 (Invitrogen) at a ratio of 1:3 according to the manufacturer's instructions (OriGene) and cultured for 24, 48, and 72 hours, respectively. The maximum transfection efficiency was observed at 48 hours.

Cell Viability Assay. Cell viability was determined by [3-(4, 5-dimethylthiazol-2-yl)-5-(3-carboxymethoxyphenyl)-2-(4-sulfophenyl)-2H-tetrazolium (MTS) assay (Promega, Madison, WI). Briefly, cells (4.5×10^3/well) were seeded in 96-well plates and infected with Ad-PPARγ or Ad-LacZ, treated with or without rosiglitazone. After treatment, 20 μL of reaction solution was added to cultured cells in 100 μL culture medium and incubated at 37°C for 1.5 hours. The optical density was measured at a wavelength of 490 nm using a Victor^3 multilabel counter (PerkinElmer, Fremont, CA).

Cell Cycle Analysis. After treatment, cells were trypsinized, washed in phosphate-buffered saline, and fixed in ice-cold 70% ethanol-phosphate-buffered saline. DNA was labeled with propidium iodide (PI). The cells were then sorted by FACScan analysis (Becton Dickinson, Franklin Lakes, NJ), and cell cycle profiles were determined using the ModFitLT software (Becton Dickinson, San Diego, CA).[7]

Cell Apoptosis Assay. Apoptosis was analyzed by PI staining for sub-G_1 DNA analysis and terminal deoxynucleotidyl transferase-mediated deoxyuridine triphosphatase nick-end labeling (TUNEL) assay.[7,14] Nuclei with clear brown staining were regarded as TUNEL-positive apoptotic cells. The apoptosis index was calculated as the percentage of TUNEL-positive nuclei after counting at least 1000 cells.[14]

Western Blot Analysis. Total protein was extracted and protein concentration was measured by the method of Bradford (DC protein assay; Bio-Rad Laboratories, Hercules, CA). Protein (30 μg) from each sample was used for Western blotting as described.[7] Bands were quantified by scanning densitometry.

PPARγ Binding Activity Assay. To determine optimal PPARγ transcription factor DNA binding activity in HCC cells, rosiglitazone was used to stimulate PPARγ/DNA binding activity. Confluent Hep3B cells were exposed to rosiglitazone at various concentrations (10, 50, and 100 μM) at various time points (1, 2, 3, 4, 6, 8, 12, 15, 24 hours) during culture. Precise PPARγ/DNA binding activity in nuclear extracts was determined by an enzyme-linked immunosorbent assay-based method (Cayman Chemical, Ann Arbor, MI). The optimal PPARγ activation was obtained in Hep3B cells under the treatment with 100 μM rosiglitazone for 3 hours.

Oligonucleotide Microarray and Analysis. Gene expression profiles of cells with highest PPARγ binding activity under treatment with rosiglitazone and control untreated cells were obtained by oligonucleotide microarray analysis using the Stanford Functional Genomics Facility and protocols (www.microarray.org). DNA microarrays contained 41,125 cDNA clones and represented approximately 24,473 unique genes. The cDNAs were amplified and spotted on glass slides in duplicate by using a robotic arrayer. Total RNA (100μg) was labeled by reverse transcription in the presence of Cy5(red)-labeled or Cy3(green)-labeled nucleotides (Amersham Biosciences, Piscataway, NJ). Two labeled RNAs were competitively hybridized to the microarray, and the signals were analyzed by using a GenePix 4000A scanner (Axon Instruments, Molecular Devices, Palo Alto, CA). Quantitation was performed by using GenePix Pro 5.0 (Axon Instruments).

Chromatin Immunoprecipitation. Chromatin immunoprecipitation (ChIP) assay was performed on Hep3B cells, infected by 75 MOI Ad-PPARγ or Ad-LacZ as control using EZ-Magna ChIP A kit (Millipore, Billerica, MA). Chromatin DNA fragments were precipitated with 10 μg PPARγ antibody (Santa Cruz

Biotechnology). The DNA was then de-crosslinked and extracted from the DNA-protein complex. The immunoprecipitated DNA was subjected to ChIP-PCR validation.

Semiquantitative ChIP-PCR. To confirm the presence of PPARγ binding on promoter targets, we performed ChIP-PCR using four known PPARγ-responsive targets, including *Acyl-coenzymeA oxidases* (*ACOX*), *phosphatase and tensin homolog* (*PTEN*), *fibronectin* (*Fn*), and *thromboxane A2 receptor* (*TBXA2R*). Immunoprecipitated DNAs were amplified with primers (Supporting Table 1) flanking the consensus sequences of the PPARγ-responsive elements. After confirming that PPARγ binds to the above promoters, we demonstrated the success of ChIP against PPARγ. Expression of *growth differentiation factor 15* (*GDF15*) promoter was detected in ChIP DNA samples with primer sequences listed in Supporting Table 1. The final PCR products were electrophoresed on 1.5% agarose gels and photographed under ultraviolet light.

Immunohistochemistry for GDF15 and Ki-67. GDF15 and Ki-67 were detected in paraffin-embedded liver sections using the specific antibodies and an avidin-biotin complex immunoperoxidase method.[14] The proliferation index was determined by counting the numbers of cells staining positive for Ki-67 as percentages of the total number of tumor cells. At least 1000 tumor cells were counted each time.

cDNA Synthesis and Reverse Transcription PCR. Total RNA was extracted from frozen liver tissues and cell pellets with RNA Trizol reagent (Invitrogen, Carlsbad, CA). The messenger RNA (mRNA) expression level of the target gene was determined by reverse transcription PCR (RT-PCR).[7]

Statistics. Data were expressed as mean ± standard deviation (SD). Nonparametric data between two groups was computed by chi-squared test or Fisher Exact test. Multiple group comparisons were made by one-way analysis of variance after Bonferroni's correction or Kruskal-Wallis test where appropriate. The difference for two different groups was determined by Mann-Whitney U test. A P value of less than 0.05 was considered statistically significant.

Results

PPARγ Insufficiency Accelerates Hepatocarcinogenesis. Because PPAR$\gamma^{-/-}$ mice were embryonically lethal, PPAR$\gamma^{+/-}$ animals and their wild-type (WT) littermates, PPAR$\gamma^{+/+}$, were studied. DEN induced HCC development at 8 months (Fig. 1A). DEN induced 62% (8/13) of liver cancer in PPAR$\gamma^{+/+}$ mice (Fig. 1B) with increased tumor prevalence in PPAR$\gamma^{+/-}$ mice (94%, 16/17, $P < 0.05$). Moreover, the average number of tumors per animal was 2.4-fold higher in PPAR$\gamma^{+/-}$ than in WT mice ($P < 0.05$; Fig. 1C). Rosiglitazone treatment significantly attenuated the number and size of HCCs in WT mice compared with the PPAR$\gamma^{+/-}$ mice (Fig. 1B,C). Thus, PPARγ insufficiency appears to enhance DEN-induced hepatocarcinogenesis in mice, while conferring refractoriness to rosiglitazone treatment. No differences in macroscopic and histologic features of HCCs were observed between WT and PPARγ-deficient mice treated with or without rosiglitazone, as evaluated by a pathologist (K.F.T.).

Proliferative activity in HCCs from WT and PPAR$\gamma^{+/-}$ mice was determined by Ki-67 immunostaining, whereas the apoptotic index was quantified using TUNEL. HCCs from PPAR$\gamma^{+/-}$ mice displayed significantly greater proliferative activity (28% ± 4.9% versus 22% ± 2.5%, $P < 0.005$; Fig. 2A-C), and reduced apoptotic cell death compared with WT littermates (1.4% ± 0.4% versus 4.8% ± 1.7%, $P < 0.001$; Fig. 2D-F).

Overexpression of PPARγ Reduces Cell Proliferation and Induces Cell Cycle Arrest in Human HCC Cells. To elucidate the role of PPARγ in human HCC cells, Hep3B was transfected with PPARγ via an adenovirus carrying PPARγ (Ad-PPARγ), or Ad-LacZ as a control. X-gal staining was used to indicate the gene transfer efficiency over 24, 48, and 72 hours. The extensive transduction (>80%) was achieved at 72 hours in the Hep3B cell line (Fig. 3A). The expression of PPARγ was markedly induced in Ad-PPARγ-treated cells in a dose-dependent manner, but not in Ad-LacZ-treated cells (Fig. 3B). Because induction of PPARγ expression was demonstrated after its agonist stimulus,[2,7] we tested the effects of rosiglitazone on expression of PPARγ. Rosiglitazone treatment of transfectants resulted in a further enhancement of PPARγ expression (Fig. 3C).

The effect of PPARγ overexpression on cell viability of Hep3B cells was then analyzed by MTS assay. Ad-PPARγ transfection suppressed cell viability in a dose-dependent and time-dependent fashion (Fig. 4A,B) compared with Ad-LacZ controls. In addition, cotreatment of Hep3B cells with Ad-PPARγ and rosiglitazone had an additive effect of reducing cell viability in Hep3B cells (Fig. 4C). Fluorescence-activated cell sorting (FACS) analysis of PPARγ-transfected Hep3B cells (Fig. 5A) revealed a significant reduction in the number of S phase cells compared to LacZ-transfected cells

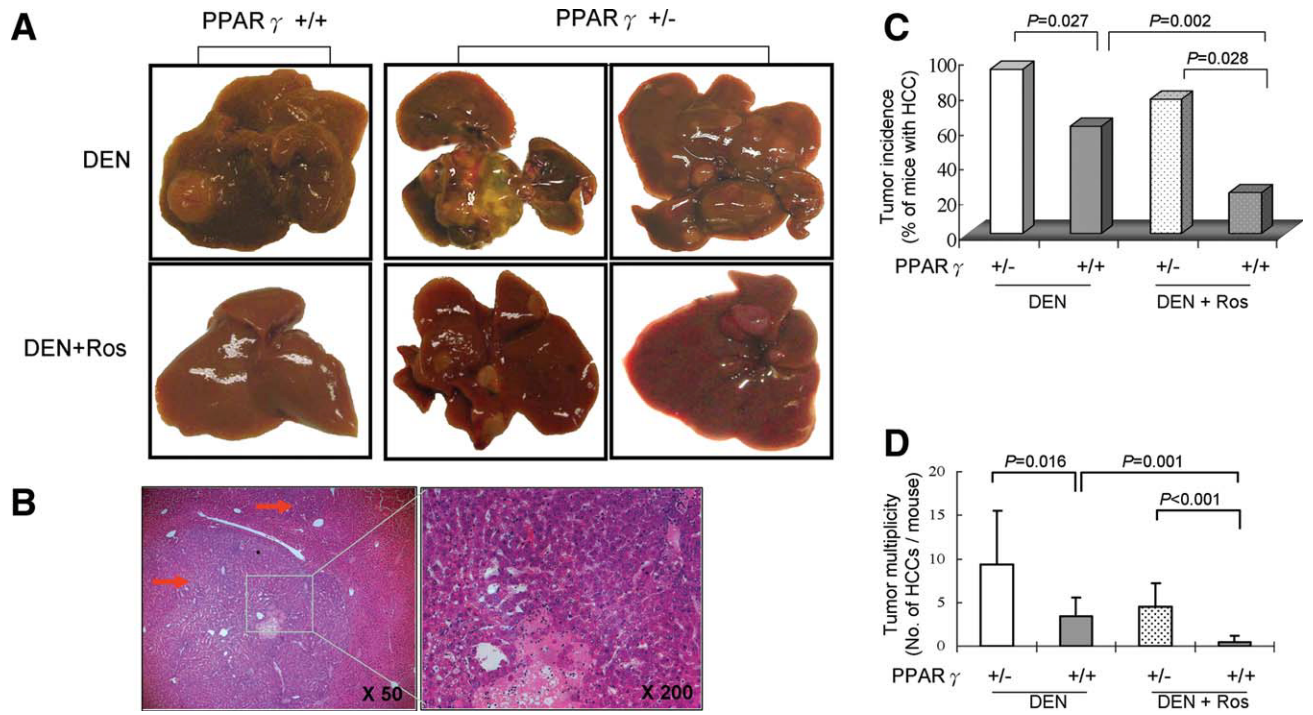

Fig. 1. PPARγ insufficiency in-creases susceptibility to DEN-induced hepatocarcinogenesis. (A) Typical gross morphology of liver tumors from DEN-treated PPARγ deficient (PPAR$\gamma^{+/-}$) or wild-type (PPAR$\gamma^{+/+}$) male mice supplemented with or without rosiglitazone (Ros) at 8 months. (B) Representative microscopic features of HCC in hematoxylin and eosin (H&E)-stained liver sections of mice. Arrows indicate microscopic HCC. (C) HCC incidence in different treatment groups, and (D) The number of HCCs per mouse was counted and expressed as mean $\pm$ SD.

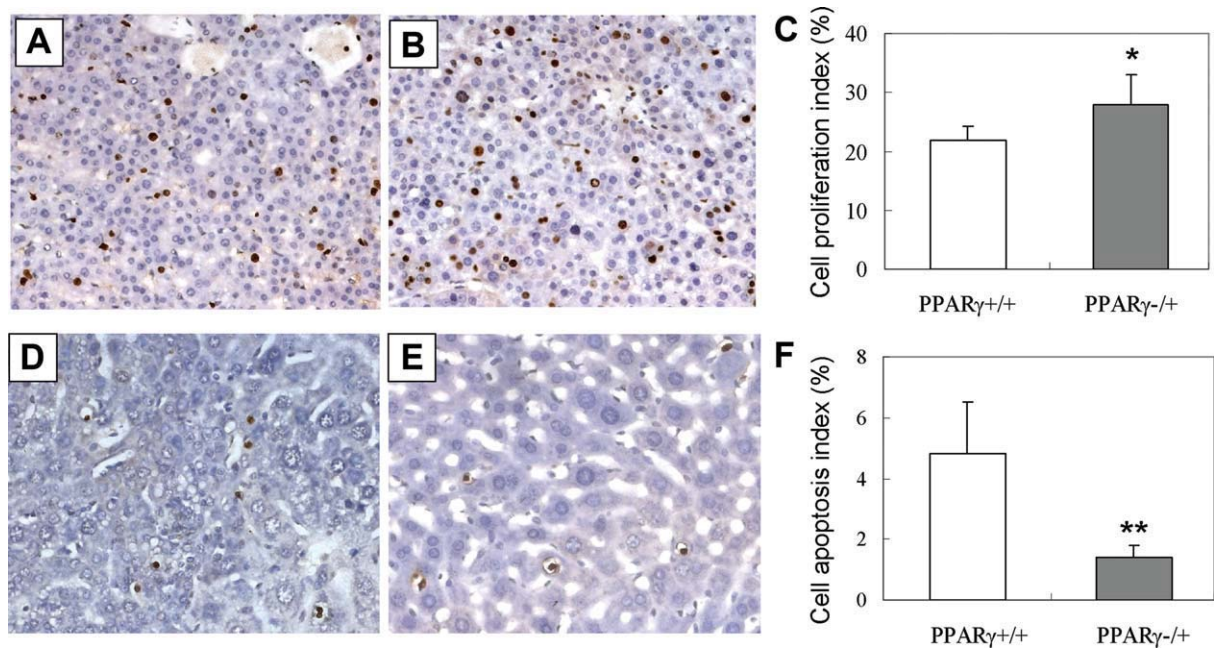

Fig. 2. (A-C) Cell proliferation in HCCs of PPAR$\gamma^{+/+}$ (A) and PPAR$\gamma^{+/-}$ (B) mice by Ki-67-positive cells. (C) Quantitative assessment of cell proliferative index by Ki-67-positive cells at $\times$400 magnification. The percentage of proliferating cells was calculated from randomly selected HCC fields. At least 1000 cells were counted in five random fields from one to four tumors per mouse, and the percentage of Ki-67-positive cells was then calculated as cell proliferative index. (D-F) Cell apoptosis in HCCs of PPAR$\gamma^{+/+}$ (D) and PPAR$\gamma^{+/-}$ (E) mice by TUNEL staining. (F) Quantitative assessment of apoptosis by TUNEL-positive cells at $\times$400 magnification. The counting method is the same as the cell proliferative index. Data are mean $\pm$ SD, 5-6 mice/group. *$P < 0.01$, **$P < 0.001$.

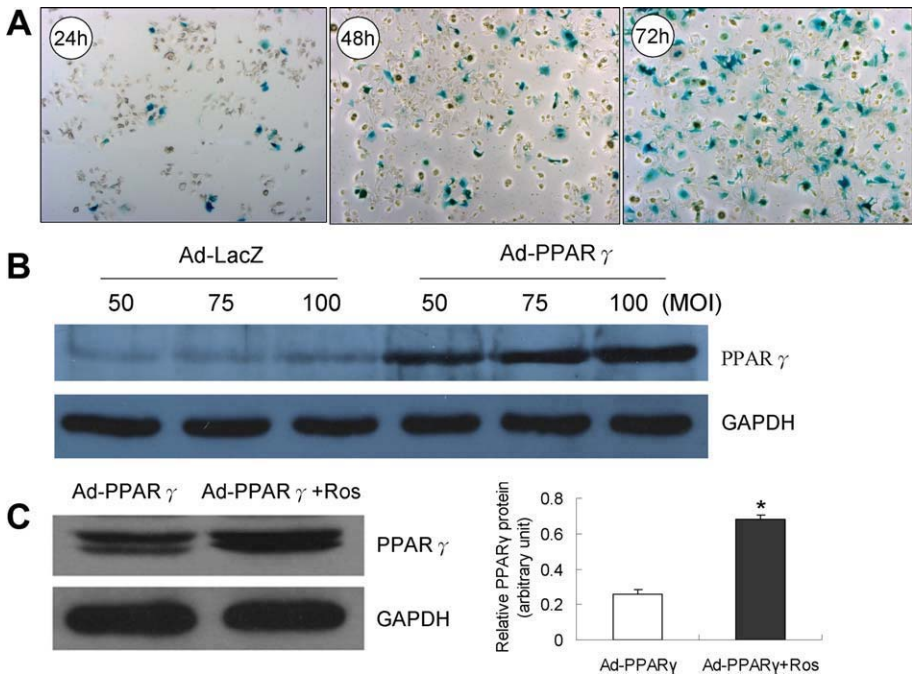

Fig. 3. Induction of PPARγ protein expression in Hep3B cells transfected with Ad-PPARγ. (A) Representative images displayed the viability of the Adv-LacZ-infected Hep3B cells (75 MOI) by X-gal staining for the indicated time periods. Ad-LacZ-transduced cells exhibited bright blue staining indicative of successful transfer and expression of the β-galactosidase gene. (B) Representative Western blots demonstrating PPARγ protein induction in Hep3B cells infected with either Ad-PPARγ or Ad-LacZ (control) at MOI of 50, 75, and 100, respectively. (C) Representative Western blots of PPARγ protein expression in Hep3B cells infected with Ad-PPARγ (75 MOI) in the presence or absence of PPARγ agonist rosiglitazone (Ros) (50 μM) at 72 hours. Glyceraldehyde 3-phosphate dehydrogenase (GAPDH) protein was used as the internal control. PPARγ protein levels (normalized to GAPDH) were measured by scanning densitometry. Data are mean $\pm$ SD (n = 3/group), $*P < 0.05$.

($P < 0.01$) (Fig. 5B). To confirm the inhibitory effect of PPARγ on cell proliferation, we evaluated proliferating cell nuclear antigen (PCNA) expression by Western blot of HCC cells and observed a diminution of PCNA by PPARγ (Fig. 5C). Concomitant with this inhibition of cell proliferation, there was a significant increase in the number of cells accumulating in the G_2/M phase ($P < 0.01$) (Fig. 5D). Other regulators of the cell cycle were also assessed. Overexpression of PPARγ in Hep3B cells induced phosphorylation of the protein phosphatases cdc25C and cdc2 (known as Cdk1), a crucial mediator in inhibiting the G_2/M phase. However, the G_0/G_1-phase regulators $p21^{Wat1/Cip1}$ and $p27^{Kip1}$ were unchanged (Fig. 5E). Thus, PPARγ overexpression reduced cell proliferative capacity with a G_2/M cell cycle arrest.

PPARγ Induces Apoptosis via Both Extrinsic and Intrinsic Apoptotic Pathways. In order to determine whether the decrease in cell proliferation observed was due to an induction of apoptosis, the cellular apoptotic

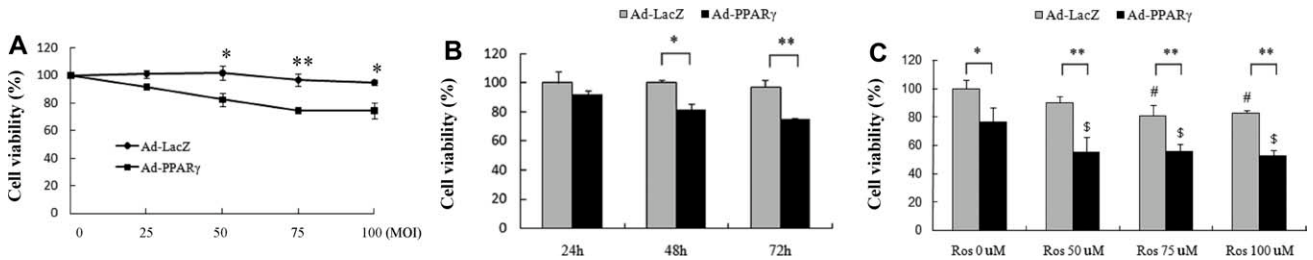

Fig. 4. PPARγ inhibited the growth of liver cancer cells. (A) Cell viability of Hep3B cells after infection with various MOIs of Ad-PPARγ or Ad-LacZ (control) for 72 hours as determined by MTS assay. $*P < 0.05$, $**P < 0.01$, cells infected with Ad-PPARγ versus infected with Ad-LacZ. (B) Cell viability of Hep3B cells after infection with Ad-PPARγ or Ad-LacZ at a MOI of 75 over time intervals. (C) Hep3B cells infected with Ad-PPARγ or Ad-LacZ at a MOI of 75 in the presence or absence of different concentrations of rosiglitazone at 72 hours. $*P < 0.05$, $**P < 0.01$, cells infected with Ad-PPARγ versus infected with Ad-LacZ; $\#P < 0.05$, rosiglitazone-treated Ad-LacZ-infected cells versus the cells infected with Ad-LacZ only; $\$P < 0.01$, rosiglitazone-treated Ad-PPARγ-infected versus the cells infected with Ad-PPARγ only. Data are means $\pm$ SD (n = 6).

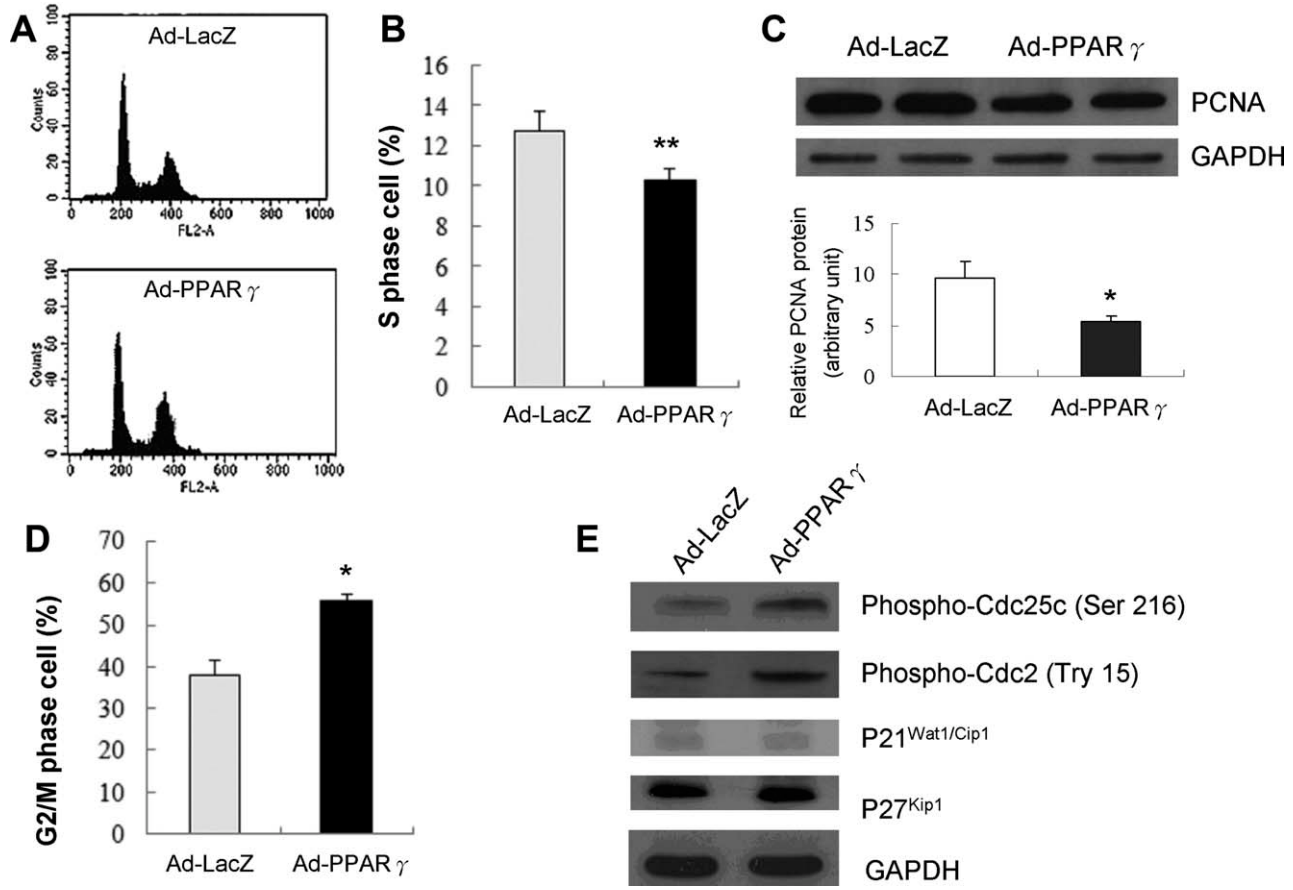

Fig. 5. Effect of PPARγ on cell proliferation and cell cycle regulation. Hep3B cells were infected with 75 MOI Ad-PPARγ or Ad-LacZ for 72 hours. (A) Representative histogram plots of the flow cytometry analysis. (B) Cell proliferation was calculated as the fraction of cells in S phase determined by flow cytometry. (C) PCNA protein expression was determined by Western blot, and GAPDH was used as loading control. (D) The number of cells in G_2/M phase was determined by flow cytometry. Values are mean ± SD from four replicate experiments. $*P < 0.05$, $**P < 0.01$. (E) Effects of PPARγ on protein expression of cell cycle regulators phospho-cdc25C, phospho-cdc2, $p21^{Wat1/Cip1}$, and $p27^{Kip1}$ by Western blot. GAPDH was used as loading control.

rate was appraised using annexin-V-fluorescein isothiocyanate (FITC)/PI by flow cytometry. The number of apoptotic cells at 72 hours following Ad-PPARγ transfection was substantially increased compared to Ad-LacZ control cells ($P < 0.001$; Fig. 6A,B); this infers that apoptosis concomitant with cell cycle arrest induced by PPARγ was a plausible cause leading to the growth inhibition in PPARγ-expressing HCC cells.

To further define the molecular basis of cell death in the tumor cells, we assessed the apoptosis markers, Fas, Bax, apoptotic protease activating factor 1 (APAF-1), P63, caspase-3, caspase-7, caspase-8, caspase-9, and nuclear enzyme poly(ADP-ribose) polymerase (PARP) by Western blot and tumor necrosis factor alpha (TNFα), TNF-related apoptosis-inducing ligand-DR4 (TRAIL-DR4), and TRAIL-DR5 by RT-PCR. Overexpression of PPARγ enhanced Fas, TNF-α, and cleaved caspase-8, which are proapoptotic mediators for the extrinsic apoptotic pathway; induced Bax and APAF-1, and cleaved caspase-9, caspase-3, caspase-7, and PARP, which are proapoptotic regulators for the intrinsic apoptotic pathway; and up-regulated p63 (Fig. 6C,D).

PPARγ Up-Regulates GDF15 Expression. There was a 10-fold increase in the abundance of GDF15 in Hep3B under PPARγ agonist (rosiglitazone) activation by cDNA expression array analysis. In order to investigate the effect of PPARγ on GDF15, Hep3B cells were transfected with Ad-PPARγ or Ad-LacZ for varying time periods. Enhanced expression of GDF15 mRNA (Fig. 7A) and protein (Fig. 7B) were observed in Ad-PPARγ-transfected cells compared with Ad-LacZ controls. This effect occurred in a time-dependent manner.

Ectopic Expression of GDF15 Suppresses Proliferation and Induces Apoptosis in Hep3B Cells. To investigate whether changes in GDF15 levels were associated with tumor suppressive properties, we

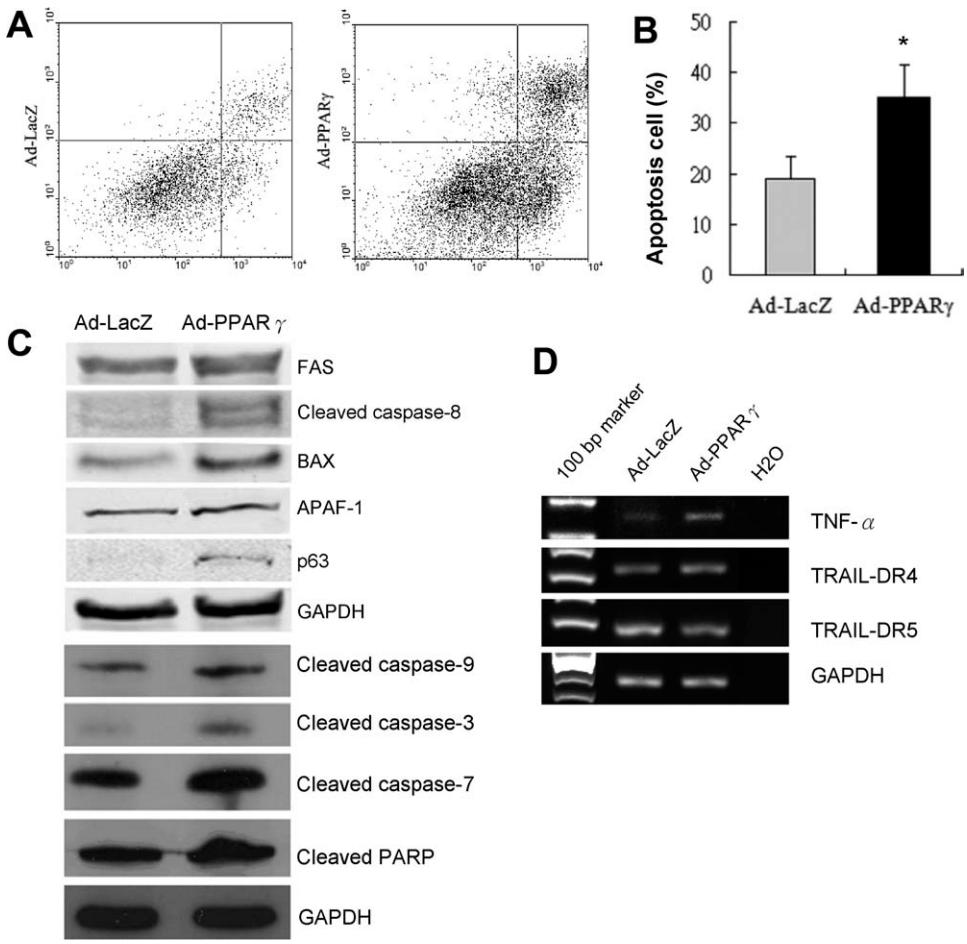

Fig. 6. PPARγ-induced cell apoptosis. Hep3B cells were infected with 75 MOI Ad-PPARγ or Ad-LacZ for 72 hours. (A) The effect of PPARγ overexpression on apoptosis was determined by FACS using annexin V apoptosis assay. (B) Annexin V-positive apoptotic cells was significantly increased in Ad-PPARγ-infected cells compared with Ad-LacZ-infected cells. Values are mean ± SD from four replicate experiments. $*P < 0.001$. (C) Protein expression of FAS, Bax, apoptotic protease activating factor 1 (APAF-1), p63, cleaved caspase-3, caspase-7, caspase-8, caspase-9, and nuclear enzyme poly(ADP-ribose) polymerase (PARP) was evaluated by Western blot. GAPDH was used as loading control. (D) The mRNA expression of TNF-α, TRIAL-DR4, and TRIAL-DR5 was examined by RT-PCR. GAPDH was used as internal control.

investigated the effect of ectopic expression of GDF15 on cell proliferation and apoptosis. Our results showed that cell viability was significantly reduced after a 48-hour transfection of pCMV/GDF15 compared with transfection of empty pCMV vector in Hep3B cells (83 ± 13 versus 100 ± 9; $P < 0.05$). Immunoblot analysis of protein extracts derived from pCMV/GDF15-transfected Hep3B cells showed a corroborative reduction in PCNA expression compared with the empty pCMV vector (Fig. 7C), whereas there was a significant enhancement in the number of apoptosis cells by flow cytometry (Fig. 7D).

PPARγ Functionally Interacts with GDF15 in Hep3B Cells and In Vivo. To evaluate whether the observed PPARγ-mediated induction of GDF15 expression was under direct modulation of the transcriptional activity of its promoter, the interaction of PPARγ with the GDF15 gene promoter was investigated by ChIP assay. Hep3B chromatin was immunoprecipitated with the anti-PPARγ antibody. PCR was used to determine the recruitment of PPARγ to the GDF15 promoter region. PPARγ was weakly constitutively bound to the GDF15 promoter in Ad-LacZ-treated cells; this recruitment was increased by Ad-PPARγ treatment (Fig. 7E). The presence of PPARγ binding on promoter targets was validated and confirmed by ChIP-PCR on four well-known PPAR-responsive targets: PTEN, ACOX, Fn, and TBXA2R (Fig. 7E).[15-18]

To ascertain the functional interaction of PPARγ and GDF15 in liver tumorigenesis *in vivo*, we examined the expression of GDF15 by immunohistochemistry in HCCs and adjacent normal liver from WT and $PPAR\gamma^{+/-}$ mice. In DEN-treated WT mice, GDF15 immunostaining was present in normal liver with comparatively weaker expression in tumor tissue (Fig. 8A). In contrast, normal hepatocytes from $PPAR\gamma^{+/-}$ mice displayed minimal GDF15 staining with a paucity of expression in corresponding HCCs (Fig. 8B). PPARγ treatment with rosiglitazone stimulated GDF15 expression by immunostaining (Fig. 8C). Immunohistochemistry findings were confirmed by Western blot (Fig. 8D). These results suggest that loss of GDF15 is associated

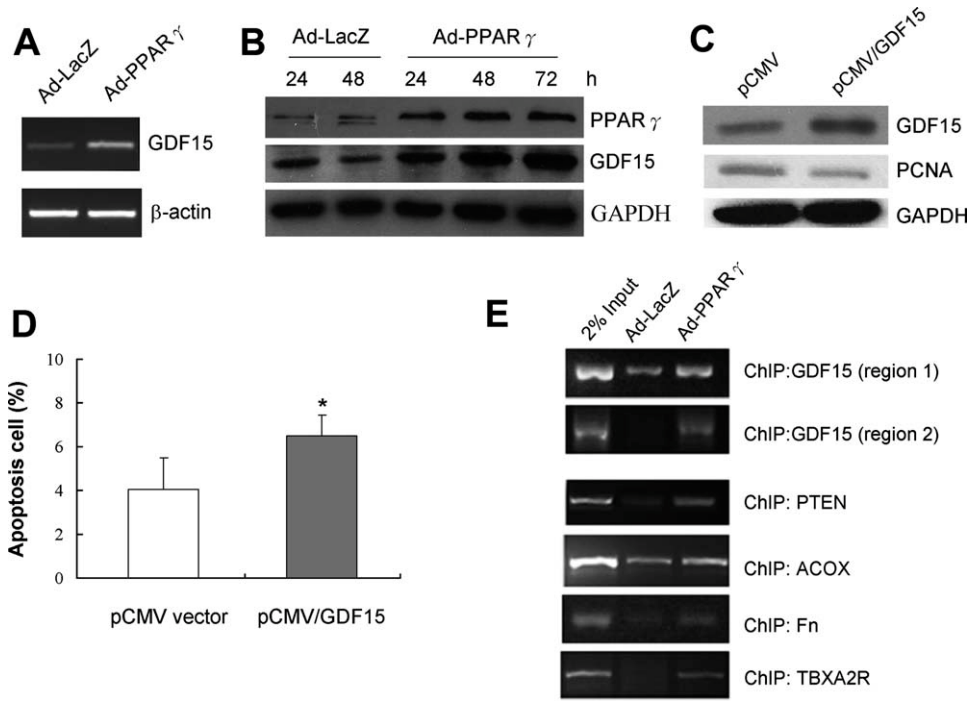

Fig. 7. (A) Semiquantitative RT-PCR evaluation of GDF15 mRNA expression in Hep3B cells transfected with Ad-PPARγ or Ad-LacZ (75 MOI) for 72 hours. (B) Immunoblots of GDF15 from Hep3B cells transfected with Ad-PPARγ or Ad-LacZ (75 MOI) at the indicated time intervals, GAPDH was used as loading control. (C) The Hep3B cells were transfected with GDF15-expressing (pCMV6/GDF15) or empty vector (pCMV6) for 48 hours; forced expression of GDF15 protein level were observed by Western blot. Concomitant with the induction of GDF15, expression of PCNA was decreased. GAPDH was used as the internal control. (D) Ectopic expression of GDF15 significantly increased apoptosis in Hep3B cells by annexin V-FITC and PI, as analyzed by flow cytometry. Values are mean $\pm$ SD from five replicate experiments. $*P < 0.05$, pCMV6/GDF15 treated versus pCMV6 vector. (E) Functional interaction between PPARγ and GDF15 promoter. Hep3B cells were treated with PPARγ (75 MOI) for 72 hours, then crosslinked with formaldehyde and lysed. The soluble chromatin was immunoprecipitated with the anti-PPARγ antibody. Two pairs of primers were designed to detect the peroxisome proliferator response element (PPRE)-containing promoter region of GDF15. To control input DNA, GDF15 promoter was amplified from the initial preparations of soluble chromatin (before immunoprecipitations). To confirm the presence of PPARγ binding on promoter targets, we also performed ChIP-PCR using four well-known PPAR-responsive targets, including phosphatase and tensin homolog (PTEN), Acyl-CoA oxidases (ACOX), fibronectin (Fn) and thromboxane A2 receptor (TBXA2R).

with liver carcinogenesis whereas restoration of GDF15 leads to the attenuation of HCC development.

Discussion

Although activation of the PPARγ signaling pathway by the agonist troglitazone has been shown to inhibit growth and induce differentiation and apoptosis in human HCC cell lines,[7] there have been no studies to mechanistically define the role of PPARγ in hepatocarcinogenesis. Using a DEN-induced murine model of HCC, we demonstrated that the loss of one PPARγ allele significantly enhanced liver carcinogenesis. Our results are consistent with other mouse models of solid organ malignancies such as stomach,[19] intestine,[20] and thyroid,[21] where PPARγ haploinsufficiency increased the susceptibility to carcinogen-induced tumors compared with WT animals. Moreover, our group has previously shown that human HCCs display impaired PPARγ expression.[7] Others have reported reduction in PPARγ protein expression in lung, breast and colon cancers, where expression was highest only in normal tissue with sequential reduction from benign to preneoplastic and malignant tissues,[22-24] implying that PPARγ regulates tumor progression. However, one report showed increased expression of PPARγ in and around the HCC tumors by immunohistochemistry.[25] This contradictory result remains to be resolved by using a specific antibody on larger samples. This study demonstrates the efficacy of rosiglitazone, a commercially available PPARγ agonist, in attenuating DEN-induced HCC. Rosiglitazone significantly suppressed HCC development only in WT mice, unlike their heterozygous littermates. Together, these findings suggest that PPARγ plays a tumor-suppressive role in hepatocarcinogenesis. Considering a recent report showing higher serum concentrations of the physiological PPARγ agonist 15-deoxy-delta(12,14)-prostaglandin J2

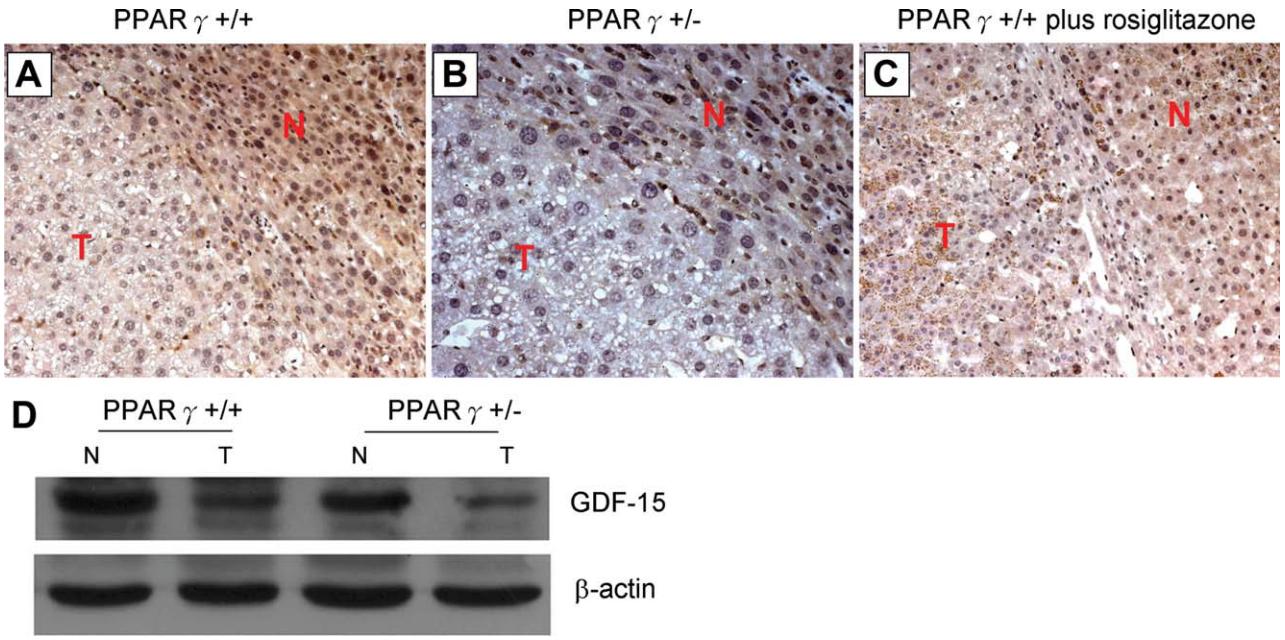

Fig. 8. (A-C) GDF15 expression by immunohistochemistry in DEN-treated WT and PPAR$\gamma^{+/-}$ HCCs and adjacent normal liver tissue at 8 months. (A) WT mice treated with DEN display intense staining of GDF15 in the adjacent normal hepatocytes, whereas loss of GDF15 expression is noted in subpopulations of neoplastic hepatocytes. (B) PPAR$\gamma^{+/-}$ mice treated with DEN exhibit decreased GDF15 immunostaining in normal hepatocytes relative to WT mice with minimal expression in HCCs. (C) In WT mice treated with DEN and rosiglitazone, expression of GDF15 was seen in HCCs. T, tumor area; N, adjacent normal liver tissue. (D) GDF15 expression in WT and PPAR$\gamma^{+/-}$ mice by Western blot.

(a natural PPARγ agonist) in patients with HCC compared with healthy controls,[26] and the fact of the interaction of PPARγ with its physiological agonist, therapeutic attempts to induce PPARγ expression may show synergistic activity with the use of PPARγ agonists for HCC therapy.

To better define the effect of endogenous transactivation of PPARγ in liver carcinogenesis, we examined its functional consequences by overexpression in the human HCC cell line Hep3B. The choice of human HCC Hep3B cells for this study was based on two observations: (1) higher transfection efficiency of Ad-PPARγ and Ad-LacZ in Hep3B compared with other HCC cell lines (e.g., HepG2), and (2) previous demonstration of rosiglitazone's efficacy in inhibiting tumor cell growth in this cell line.[7] In this study, increased PPARγ expression led to the inhibition of cell growth in a time-dependent and dose-dependent manner. In the presence of the PPARγ agonist rosiglitazone, a more pronounced diminution in Hep3B cell viability was observed, lending further support to its role in inhibiting HCC development. To further investigate the mechanism by which PPARγ regulates cell growth, we performed FACS; cell cycle distribution analysis revealed significantly more Ad-PPARγ cells were arrested in the G_2/M phase, with a concomitant reduction in cellular proliferation compared with Ad-LacZ controls.

To explore the molecular mechanism underlying G_2/M phase arrest, we studied the regulatory proteins that controlled the G_2/M checkpoint in the cell cycle. G_2/M phase arrest by PPARγ was associated with Cdc25C phosphatase activation by Ser216 phosphorylation. After phosphorylation, Cdc25C is known to bind to members of the 14-3-3 proteins, sequestering it into the cytoplasm, thereby preventing premature mitosis.[27] Cdc25C also plays a critical role in the dephosphorylation of Cdc2 on Tyr15; Cdc2 is a major kinase involved in G_2/M cell cycle control and the entry of all eukaryotic cells into mitosis,[28] and inhibiting Cdc25C activity may result in the Tyr15 phosphorylation and inactivation of Cdc2. Cell cycle arrest caused by the overexpression of p53 has been associated with induction of p21 and p27.[29] Troglitazone was associated with induction of p27, but not p21 in Hep3B cells.[7] The reason for the inability of enhanced PPARγ to induce p21 and p27 in Hep3B cells could be explained by p53 deletion in this cell line. The mechanism of troglitazone-mediated p27 induction is likely to be independent of PPARγ.

A disruption in the balance between cellular proliferation and apoptosis may contribute to the initiation and progression of cancer.[30] In contrast, resistance of apoptosis is a likely requirement for cancer cell maintenance.[31] The induction of apoptosis in Hep3B cells by PPARγ was also observed concomitantly with the

inhibition of cellular proliferation, whereby apoptosis was executed by two major apoptotic pathways: the extrinsic death receptor-triggered apoptotic pathway and the intrinsic mitochondrial caspase-dependent pathway. PPARγ enhanced expression of Fas and TNF-α, which initiated an external signal and activated the extrinsic apoptosis pathway through the Fas-associated death domain. This pathway is mediated by activation of caspase-8, an initiator caspase, followed by direct cleavage of downstream effector caspases. Meanwhile, the intrinsic apoptotic pathway was also stimulated by PPARγ, which induced the transcription of Bax and the release of caspase-activating proteins into the cytosol, resulting in the activation of the APAF-1. The APAF-1 then formed an activation complex with caspase-9. The activated caspase-9 triggered downstream caspase effectors including caspase-3 and caspase-7 to initiate a caspase cascade. These effectors further stimulated the proteolytic cleavage of PARP, which facilitates cellular disassembly and undergoes apoptosis. Overexpression of PPARγ in multiple myeloma cells[32] and thyroid carcinoma cells[31] has also been shown to markedly affect their susceptibility to apoptosis via increased caspase-3 activity and PARP cleavage.[32] The tumor suppressor gene p63, a sensor of DNA damage,[33] was up-regulated upon PPARγ stimulation. Thus, heightened PPARγ expression may diminish HCC development by up-regulating apoptotic cell death pathways.

Oligonucleotide microarray analysis was used to identify potential novel target genes of PPARγ. Among the genes up-regulated by PPARγ, *GDF15* (also known as NAG1, *MIC-1*, *PLAB*), a member of the TGF-β superfamily, was predominant. Increased expression of *GDF15* protein was confirmed by Western blot in Hep3B cells transfected with Ad-PPARγ. Overexpression of *GDF15* in Hep3B cells led to inhibition of cell growth, proliferation and induction of apoptosis. Similar effects have been observed in several types of cancer cells such as lung,[34] prostate,[35] and colon cancer.[36] Further, transfection of *GDF15* cDNA in a xenograft animal model has resulted in the inhibition of lung cancer and glioblastoma development.[31,37] These findings suggest a possible mechanism by which PPARγ suppresses HCC growth. Using the observed interaction between PPARγ and *GDF15* promoter in a ChIP assay, we validated and confirmed the presence of PPARγ binding on promoter targets of four known response genes PTEN, ACOX, Fn, and TBXA2R. Because *GDF15* is considered a tumor suppressor gene that is capable of inducing transcriptional up-regulation of other antitumorigenic genes, the precise downstream pathways by which it mediates such effects are worthy of future studies. Having observed the direct interplay of PPARγ and GDF15 *in vitro*, we studied PPARγ and GDF15 protein expression in *vivo*. Down-regulation of GDF15 appears to be associated with HCC development and such low levels of expression may be reversed by exogenous rosiglitazone in WT mice. These observations were consistent with *in vitro* findings in Hep3B cells.

In conclusion, PPARγ can function as a tumor-suppressor gene in hepatocarcinogenesis. PPARγ inhibited tumor cell growth through suppressing cell proliferation, inducing G_2/M arrest and apoptosis, and up-regulating GDF15.

References

1. Parkin DM, Bray F, Ferlay J, Pisani P. Global cancer statistics, 2002. CA Cancer J Clin 2005;55:74-108.
2. Koeffer HP. Peroxisome proliferators-activated receptor gamma and carcinomas. Clin Cancer Res 2003;9:1-9.
3. Sertznig P, Seifert M, Tilgen W, Reichrath J. Present concepts and future outlook: function of peroxisome proliferator-activated receptors (PPARs) for pathogenesis, progression, and therapy of cancer. J Cell Physiol 2007;212:1-12.
4. Kopelovich L, Fay JR, Glazer RI, Crowell JA. Peroxisome proliferator-activated receptor modulators as potential chemopreventive agents. Mol Cancer Ther 2002;1:357-363.
5. Grommes C, Landreth GE, Heneka MT. Antineoplastic effects of peroxisome proliferator-activated receptor gamma agonists. Lancet Oncol 2004;5:419-429.
6. Ondrey F. Peroxisome proliferator-activated receptor gamma pathway targeting in carcinogenesis: implications for chemoprevention. Clin Cancer Res 2009;15:2-8.
7. Yu J, Qiao L, Zimmermann L, Ebert MP, Zhang H, Lin W, et al. Troglitazone inhibits tumor growth in hepatocellular carcinoma in vitro and in vivo. HEPATOLOGY 2006;43:134-143.
8. Hsu MC, Huang CC, Chang HC, Hu TH, Hung WC. Overexpression of Jab1 in hepatocellular carcinoma and its inhibition by peroxisome proliferator-activated receptorγ ligands in vitro and in vivo. Clin Cancer Res 2008;14:4045-4052.
9. Akiyama TE, Sakai S, Lambert G, Nicol CJ, Matsusue K, Pimprale S, et al. Conditional disruption of the peroxisome proliferator-activated receptor gamma gene in mice results in lowered expression of ABCA1, ABCG1, and apoE in macrophages and reduced cholesterol efflux. Mol Cell Biol 2002;22:2607-2619.
10. Borbath I, Horsmans Y. The role of PPARgamma in hepatocellular carcinoma. PPAR Res 2008;2008:209520.
11. Koga H, Sakisaka S, Harada M, Takagi T, Hanada S, Taniguchi E, et al. Involvement of $p21^{WAF1/Cip1}$, $p27^{Kip1}$, and $p18^{INK4c}$ in troglitazone-induced cell-cycle arrest in human hepatoma cell lines. HEPATOLOGY 2001;33:1087-1097.
12. Koga H, Harada M, Ohtsubo M, Shishido S, Kumemura H, Hanada S, et al. Troglitazone induces $p27^{Kip1}$-associated cell-cycle arrest through down-regulating Skp2 in human hepatoma cells. HEPATOLOGY 2003;37:1086-1096.
13. Blanquicett C, Roman J, Hart CM. Thiazolidinediones as anti-cancer agents. Cancer Ther 2008;6:25-34.
14. Yu J, Tao Q, Cheung KF, Jin H, Poon FF, Wang X, et al. Epigenetic identification of ubiquitin carboxyl-terminal hydrolase L1 as a functional tumor suppressor and biomarker for hepatocellular carcinoma and other digestive tumors. HEPATOLOGY 2008;48:508-518.
15. Guo Y, Jolly RA, Halstead BW, Baker TK, Stutz JP, Huffman M, et al. Underlying mechanisms of pharmacology and toxicity of a novel PPAR

agonist revealed using rodent and canine hepatocytes. Toxicol Sci 2007; 96:294-309.
16. Han S, Ritzenthaler JD, Rivera HN, Roman J. Peroxisome proliferator-activated receptor-gamma ligands suppress fibronectin gene expression in human lung carcinoma cells: involvement of both CRE and Sp1. Am J Physiol Lung Cell Mol Physiol 2005;289:L419-L428.
17. Teresi RE, Planchon SM, Waite KA, Eng C. Regulation of the PTEN promoter by statins and SREBP. Hum Mol Genet 2008;17:919-928.
18. Coyle AT, O'Keeffe MB, Kinsella BT. 15-Deoxy $\Delta^{12,14}$-prostaglandin J_2 suppresses transcription by promoter 3 of the human thromboxane A_2 receptor gene through peroxisome proliferator-activated receptor γ in human erythroleukemia cells. FEBS J 2005;272:4754-4773.
19. Lu J, Imamura K, Nomura S, Mafune K, Nakajima A, Kadowaki T, et al. Chemopreventive effect of peroxisome proliferator-activated receptor gamma on gastric carcinogenesis in mice. Cancer Res 2005;65:4769-4774.
20. McAlpine CA, Barak Y, Matise I, Cormier RT. Intestinal-specific PPARgamma deficiency enhances tumorigenesis in ApcMin/+ mice. Int J Cancer 2006;119:2339-2346.
21. Kato Y, Ying H, Zhao L, Furuya F, Araki O, Willingham MC, et al. PPARgamma insufficiency promotes follicular thyroid carcinogenesis via activation of the nuclear factor-kappaB signaling pathway. Oncogene 2006;25:2736-2747.
22. Sasaki H, Tanahashi M, Yukiue H, Moiriyama S, Kobayashi Y, Nakashima Y, et al. Decreased perioxisome proliferator-activated receptor gamma gene expression was correlated with poor prognosis in patients with lung cancer. Lung Cancer 2002;36:71-76.
23. Mueller E, Sarraf P, Tontonoz P, Evans RM, Martin KJ, Zhang M, et al. Terminal differentiation of human breast cancer through PPAR gamma. Mol Cell 1998;1:465-470.
24. Bogazzi F, Ultimieri F, Raggi F, Russo D, Viacava P, Cecchetti D, et al. Changes in the expression of the peroxisome proliferator-activated receptor gamma gene in the colonic polyps and colonic mucosa of 27 acromegalic patients. J Clin Endocrinol Metab 2003;88:3938-3942.
25. Schaefer KL, Wada K, Takahashi H, Matsuhashi N, Ohnishi S, Wolfe MM, et al. Peroxisome proliferator-activated receptor gamma inhibition prevents adhesion to the extracellular matrix and induces anoikis in hepatocellular carcinoma cells. Cancer Res 2005;65:2251-2259.
26. Gressner OA, Gao C, Rehbein K, Lahme B, Siluschek M, Berg T, et al. Elevated concentrations of 15-deoxy-Delta12,14-prostaglandin J2 in chronic liver disease propose therapeutic trials with peroxisome proliferator activated receptor gamma-inducing drugs. Liver Int 2009;29: 730-735.
27. Kumagai A, Yakowec PS, Dunphy WG. 14-3-3 proteins act as negative regulators of the mitotic inducer Cdc25 in Xenopus egg extracts. Mol Biol Cell 1998;9:345-354.
28. Perry JA, Kornbluth S. Cdc25 and Wee1: analogous opposites? Cell Div 2007;2:12.
29. Vogelstein B, Lane D, Levine AJ. Surfing the p53 network. Nature 2000;408:307-310.
30. Evan GI, Vousden KH. Proliferation, cell cycle and apoptosis in cancer. Nature 2001;411:342-348.
31. Martelli ML, Iuliano R, Le Pera I, Sama' I, Monaco C, Cammarota S, et al. Inhibitory effects of peroxisome poliferator-activated receptor gamma on thyroid carcinoma cell growth. J Clin Endocrinol Metab 2002;87:4728-4735.
32. Garcia-Bates TM, Bernstein SH, Phipps RP. Peroxisome proliferator-activated receptor gamma overexpression suppresses growth and induces apoptosis in human multiple myeloma cells. Clin Cancer Res 2008;14: 6414-6425.
33. Flores ER. The roles of p63 in cancer. Cell Cycle 2007;6:300-304.
34. Chen YL, Lin PC, Chen SP, Lin CC, Tsai NM, Cheng YL, et al. Activation of nonsteroidal anti-inflammatory drug-activated gene-1 via extracellular signal-regulated kinase 1/2 mitogen-activated protein kinase revealed a isochaihulactone-triggered apoptotic pathway in human lung cancer A549 cells. J Pharmacol Exp Ther 2007;323: 746-756.
35. Liu T, Bauskin AR, Zaunders J, Brown DA, Pankurst S, Russell PJ, et al. Macrophage inhibitory cytokine 1 reduces cell adhesion and induces apoptosis in prostate cancer cells. Cancer Res 2003;63:5034-5040.
36. Baek SJ, Kim JS, Jackson FR, Eling TE, McEntee MF, Lee SH. Epicatechin gallate-induced expression of NAG-1 is associated with growth inhibition and apoptosis in colon cancer cells. Carcinogenesis 2004;25: 2425-2432.
37. Albertoni M, Shaw PH, Nozaki M, Godard S, Tenan M, Hamou MF, et al. Anoxia induces macrophage inhibitory cytokine-1 (MIC-1) in glioblastoma cells independently of p53 and HIF-1. Oncogene 2002; 21:4212-4219.